



## A new method to determine the Young's modulus of refractory materials

Emmanuel de Bilbao, Eric Blond, Claire Michel, Thierry Cutard, N. Schmitt, J. Poirier

### ► To cite this version:

Emmanuel de Bilbao, Eric Blond, Claire Michel, Thierry Cutard, N. Schmitt, et al.. A new method to determine the Young's modulus of refractory materials. *Interceram*, 2010, 59 (1), pp.34-38. hal-00567765

**HAL Id: hal-00567765**

**<https://hal.science/hal-00567765>**

Submitted on 12 Nov 2018

**HAL** is a multi-disciplinary open access archive for the deposit and dissemination of scientific research documents, whether they are published or not. The documents may come from teaching and research institutions in France or abroad, or from public or private research centers.

L'archive ouverte pluridisciplinaire **HAL**, est destinée au dépôt et à la diffusion de documents scientifiques de niveau recherche, publiés ou non, émanant des établissements d'enseignement et de recherche français ou étrangers, des laboratoires publics ou privés.

# A New Method to Determine the Young's Modulus of Refractory Materials

## 1 Introduction

The high-temperature industry constantly aims for a better process design and a better energy efficiency. It requires an optimized design of refractory structures to protect the steel casing of the installations from containing hot processes. Up to now, the design of refractory linings has been conducted in conventional ways. This approach has allowed actual progress but does not enable any more presently, and considerably increases the time and cost due to the trial-and-error method used. It is more and more promising to develop numerical simulation methods for refractory structures under thermo-mechanical loading. These numerical simulation methods require the knowledge of the thermo-mechanical properties of the refractory materials. In particular, the oldest parameters to classify materials are

the Young's modulus usually known as Modulus of Elasticity (MOE) and the tensile strength limit, also known as Modulus of Rupture (MOR). They particularly are relevant because ceramics exhibit an elastic and brittle mechanical behaviour in a large temperature range. Moreover, their ratio, in conjunction with the thermal expansion, increases the thermal shock resistance which is a parameter of interest for high temperature applications. Even if this behaviour becomes more complicated for refractory especially at high temperature with the apparition of asymmetric creep behaviour [1], the consideration of the evolution of the Young's modulus with the temperature is the first step towards non-linear thermo-mechanical simulation.

The experimental methods for the determination of the Young's modulus require an utmost care, and are not easy to interpret due to the following reasons:

- The refractory are multi-component and heterogeneous ceramics.
- The thermo-mechanical behaviour of refractory materials is not only elastic but also shows a large non-linear zone.

Many tests have been designed to measure the MOE. There exists a well-known dis-

crepancy between the results obtained from each classical apparatus (i.e. tensile, compressive, bending, ultrasonic, pulse).

Obviously, whatever is the experimental device for the measurement of the MOE, it is easier to handle it for homogeneous materials than for heterogeneous ones where measurement devices have to be designed to determine the average elastic modulus [2]. For tensile tests, for instance, the sample has to be held to avoid strain localisation and single crack propagation induced by the heterogeneity of the material such as concrete [3–4]. Furthermore, for the characterization of refractory, the experimental set-up must withstand high temperature and eventually controlled atmospheres. A particular attention has to be paid to obtain good alignment between the sample axis and the machine axis to minimize bending effects even during the heating-up [5]. Compression, namely the uniaxial crushing test, is easier to handle but the effect of bending has also to be minimized [2]. Moreover, physical deformation mechanisms in compression and tensile test are different. According to [2] these phenomena account for the significant discrepancy observed between Young's modulus deduced from both

<sup>1</sup> Institut PRISME, Polytech'Orléans, 8 rue Léonard de Vinci, 45072, Orléans Cedex 2, France

<sup>2</sup> Institut CLEMENT ADER, École des Mines d'Albi-Carmaux, Campus Jarlard – 81013 Albi CT Cedex 09, France

<sup>3</sup> LMT-Cachan, 61 av Président Wilson, 94230 Cachan, France

<sup>4</sup> CEMHTI, 1d avenue de la recherche scientifique, 45071 Orléans Cedex 2, France

tests. To bypass these difficulties, ultrasonic tests allow the determination of the elastic modulus from the measurement of longitudinal and shearing wave velocities [6]. Specific technique has been developed to measure the modulus at high temperatures [7]. Nevertheless, discrepancies between tensile and ultrasonic measurements were observed. For ten years, digital image correlation techniques also have been widely used in experimental mechanics. Strain measurements carried out on refractory materials at ambient temperature have shown that this method is useful to quantify the low strain levels characterizing the refractory during the quasi-static test [8]. But now, it has to be performed at a high temperature while remaining simply and versatile.

Three-point bending test [9] is widely used in the refractory field because it is easier to conduct in comparison to the tensile or compressive one. It consists of a bending of a beam test piece, whereby the test piece is supported on bearings near its ends, and a central force is applied. The Young's modulus is estimated by measurement of the deflection of the sample thanks to a linear variable displacement transducer (LVDT) and by using classical theory of elastic beam [10–11]. Moreover, the flexural strength or tensile strength (i.e. MOR) can be estimated, too. When the span to the height of the sample ratio is small, the shear effect has to be taken into account [2]. Hence, a four-point bending test is performed rather than a three-point bending test, because pure bending moment is applied to the middle part of the sample. Nevertheless, results strongly depend on the experimental set-up. The elastic modulus might not be estimated with a good accuracy due to the low deflection of the refractory materials [5].

The purpose of this paper is to improve the evaluation of the Young's modulus using the classical bending test without any change of set-up. Indeed, whatever are the design choices for the high temperature bending

devices, the origin of the experimental artefact is the same (i.e. device deflection, contact crushing). They just are different in magnitude. Moreover, as good as the bending device can be, the discrepancy between the Young's modulus obtained by other tests and the bending test is still being present. So, it seems more promising to recast the processing of the deflection measurement and not the device itself.

The first section of this paper describes the materials and the experimental set-up used for the bending test. The following section outlines the new data processing for the determination of the Young's modulus. Finally, tests carried out on different materials are presented in the last part of this paper. And the new characterisation of the Young's modulus implementation is applied. Although the new method presented in this paper is applied on refractory materials, it is worth mentioning that it can be used to determine the Young's modulus of any material.

## 2 Material and experimental methods

### 2.1 Materials

This contribution has been performed in the framework of a French ANR project dealing with the degradation of refractory materials used in waste-to-energy facilities (ANR project DRUIDE). The combustion chambers of the waste-to-energy facilities are composed of SiC refractory lining covering metallic tubes in which high-pressure water circulates. Due to their high thermal conductivity SiC based refractory materials protect the metallic casing against high-temperature corrosion and promote the thermal transfer from flue gas. In service the SiC refractory lining is exposed to thermo-chemo-mechanical loading which can lead to frequent degradations by means of cracking, spalling or damage of refractory materials. To develop the method proposed, three different materials were considered: two SiC based refractory materials used in waste-to-

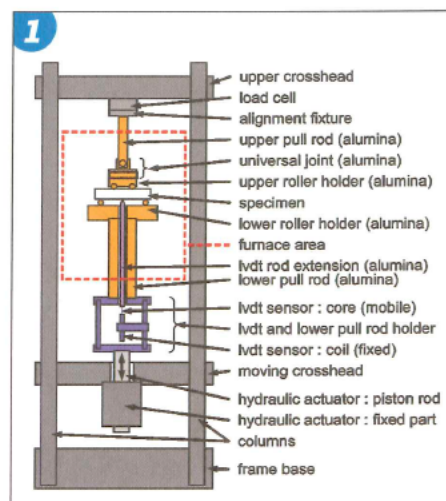


Fig. 1 • Universal testing machine and high temperature four-point bending test

energy facilities, and an alumina alloy. The alumina alloy with copper and magnesium (2024, AU4G) was used as a reference material in order to test the experimental device and to test the proposed method of measurement. Indeed, the homogeneous, elastic and linear behaviour of alumina alloy in a large range of stress allows to compare the experimental curve with the theoretical straight line and to compare the value of the Young's modulus finally obtained in comparison to the classical reference for alumina alloy: 70 GPa.

The two SiC based refractory materials are of two different natures: One is a low cement castable (LCC), while the other one is a shaped refractory material obtained by isostatic pressing and firing. The LCC is manufactured by CALDERYS and referred as SF60. It consists of 60 mass-% of SiC aggregates. After being supplied as shaped bricks, it was cured by heating at a temperature of 110 °C for 48 hours. It has been observed that the SiC aggregates with a grain size of up to 3 mm are embedded in a matrix composed of a calcium-alumina cementitious phase and of other silico-alumina phases [12]. The shaped refractory material is manufactured by HAASSER, referred as HCS90. It is composed of 90 mass-% of SiC aggregates with a grain size of up to 5 mm in a silica based bound phase. The material data are listed in Table 1.

### 2.2 Experimental method

The four-point bending tests are carried out using a MTS 810 universal testing machine (Fig. 1). A specific device has been set up and installed in a high-temperature furnace (1,600 °C). A force is applied to the sample by means of four lamina rollers (Fig. 2). The two lower alumina rollers are 125 mm spaced and supported by a fixed

Table 1 • Material data				
Material		SF60	HSC90	
Chemical analysis / mass- %	CaO	1.4	2.5	Al <sub>2</sub> O <sub>3</sub>
	Cement	5	7.3	SiO <sub>2</sub>
	Si-Al phases	35	0.2	Fe <sub>2</sub> O <sub>3</sub>
	SiC	60	90 ± 2	SiC
	Water	6.9		
Bulk density / g/cm <sup>3</sup>		2.58 ± 0.02	2.65 ± 0.05	
Apparent porosity / %		15.6 ± 0.4	15 ± 2	



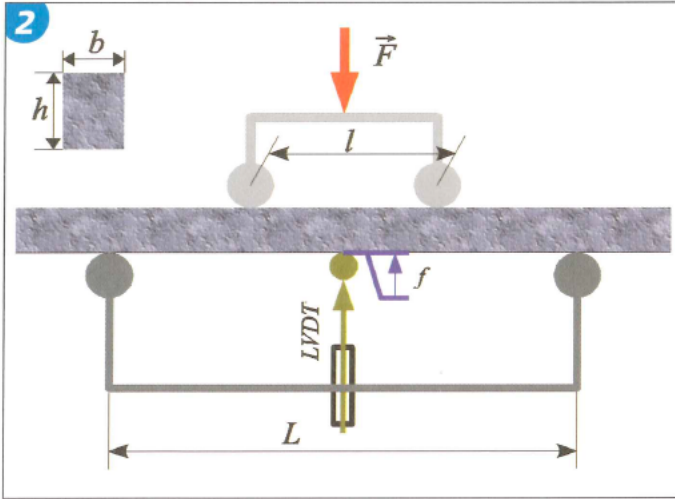


Fig. 2 • Four-point bending test

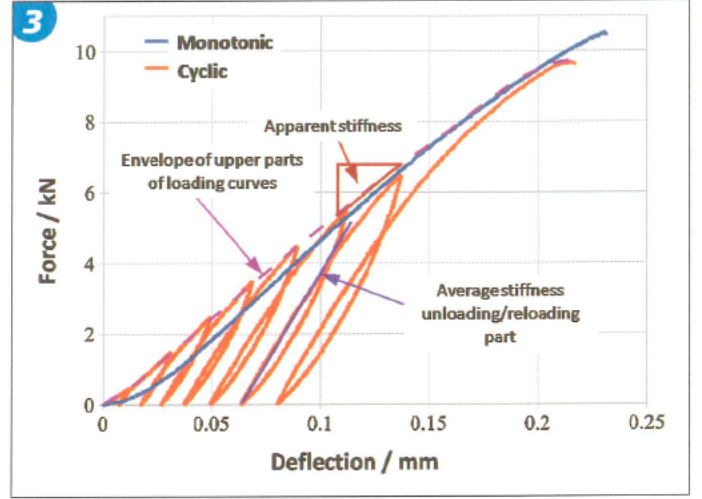


Fig. 3 • Force-deflection curves of four-point bending test of the SF60 performed at a temperature of 800 °C (monotonic and cyclic tests)

base. The two upper ones have a distance 45 mm and are supported by a freely rotating universal joint. The specimens have a length of 150 mm. For the alumina alloy the cross-section is 25 mm × 25 mm; for the refractory material the cross-section is 40 mm × 40 mm. The lower and upper faces of the samples are ground in order to obtain a parallax error lower than 0.05 mm between these two faces. The measurement of the sample deflection is performed by a LVDT coupled with a fine alumina rod in contact with the central point of the sample lower face. The applied force and the beam deflection are recorded during the test.

Figure 3 exhibits the force-deflection curves of a monotonic and a cyclic four-point bending test carried out for SF60 at a temperature of 800 °C. Regarding the monotonic test, the curve shows a slight non-linear part at the early beginning which is classically explained by the setting of the whole device. The displacement of 0.04 mm reveals a linear part which could indicate a linear elastic behaviour with an elastic module equal to 9 GPa. On the other hand, the cyclic curve reveals the existence of a residual deflection with a hysteresis due to a non-elastic behaviour. It is obvious that the non-elastic behaviour can be explored only during a cyclic test. The monotonic test cannot reveal this type of behaviour. Moreover, it should be noted that the linear monotonic curve is close to the envelope of the upper parts of the cyclic-loading curves. It follows that using the tangent line of the monotonic curve only gives an “apparent linear stiffness”. For the three last cycles the curve reveals a slight reduction of the apparent stiffness. This phenomenon could be due to the damage of the refractory material. It is worth mentioning that the average slope of the unloading-reloading loop

seems to be constant over the cycles. Furthermore, this slope is clearly higher than that of the monotonic test previously named “apparent stiffness”. Regarding this fact we have to try to get to the bottom of the physical meaning of the “apparent stiffness”.

The cyclic four-point bending test was carried out for the alumina alloy (2024) specimen at room temperature in order to understand the non-linear behaviour of the previous curve. Indeed, this material has a suitable linear elastic behaviour. Any hysteretic behaviour should not be observed.

Figure 4 exhibits the force-deflection curve of this second test. It should be noted that the cyclic curve shows the same behaviour as the curve for the refractory material obtained previously despite the well-known linear elastic behaviour. It confirms that the non-linearity of the curve also is induced by the set-up and the measurement. Furthermore, the higher the load, the closer the apparent stiffness obtained during loading and unloading. This implies that the phenomena – which generate the difference between the evolutions of the monotonic and cyclic stiffness versus the cycles – vanish with increasing number of cycles.

This observation justifies the classical procedure of compressive tests in civil-engineering: performing three (low) load-unload cycle to crush the plane contact between apparatus and sample before carrying out the actual test.

### 3 Young's modulus determination: a new approach

By applying the elastic beam theory Young's modulus usually is calculated as follows [5]:

$$E = \frac{P}{f} \frac{1}{8bh^3} (L-l) (2L^2 + 2Ll - l^2) \quad (1)$$

where  $P$  is the applied force;  $b$  and  $h$  are the width and the thickness of the sample, respectively;  $L$  and  $l$  are the distances between the lower and the upper loading rollers, respectively.  $f$  is the deflection measured at the central point of the lower face of the sample. Following the observations for the stiffness the calculation of the elastic modulus by means of equation (1) may result to different values depending on the slope extracted from the experimental curve. Indeed, monotonic loading only supplies the “linear apparent stiffness” as shown in Fig. 3. It is obvious that the calculation of the Young's modulus by means of the slopes within the loading curves of the cyclic test supplies higher values than the one deduced from the monotonic test. The unloading slope gives a third different value. The only important question is: which part of the experimental curve enables a more accurate characterization of the elastic behaviour?

The measured deflection is the relative displacement between two points: a reference point taken in the device and another “moving” point on the sample (usually the middle point of the lower or upper face). Then, this displacement is not exactly equal to the deflection calculated by means of the beam theory, but is the sum of every strain occurring through the chain links of the test device. Therefore, the displacement measured by the LVDT is the sum of the sample deflection, device compressive strain, and contact crushing, which may be elastic or not. Finally, the measured deflection can be split into four components (Fig. 5):

$$f = f_{su} + f_{co} + f_{ne} + f_e \quad (2)$$

where  $f_{su}$  is the elastic deflection of the set-up;  $f_{co}$  is the elastic part of the crushing in the contact area;  $f_{ne}$  is the non-elastic part of the measured displacement (i.e. indistinct

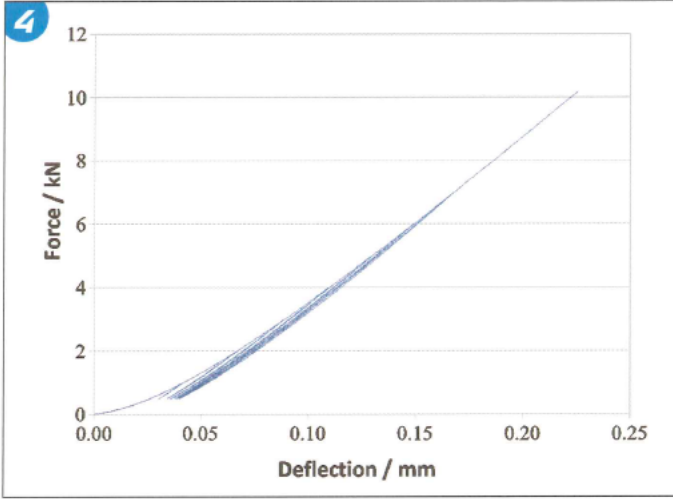


Fig. 4 • Force-deflection curve of four-point cyclic bending test of alumina at room temperature

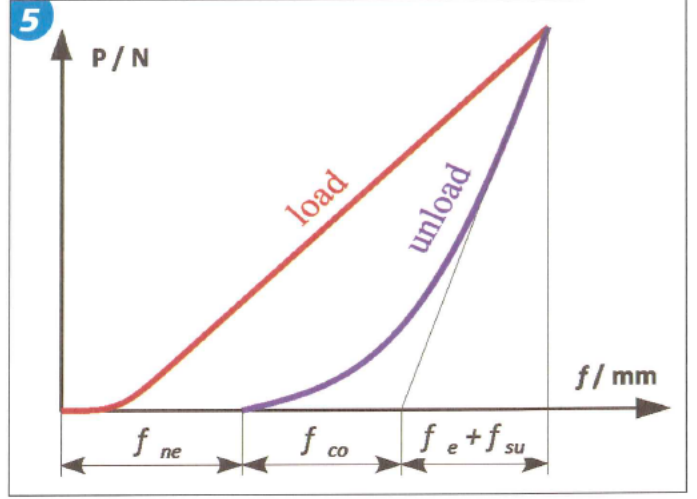


Fig. 5 • Deflection split during unloading

sum of plastic deflection of the sample, contacts, set-up), and  $f_e$  is the elastic deflection of the tested material. It is obvious that only the last component is of interest to calculate the elastic modulus.

Regarding the elastic crushing due to contact, Hertz's hypothesis applied to the contact of a rigid cylinder onto an elastic half-space plane leads to the following relationship [13–14]:

$$F_c = K_c f_{co}^n, \quad n > 1 \quad (3)$$

where  $F_c$  is the normal force applied to the contact;  $f_{co}$  is the displacement of the two solids towards each other due to the crushing, and  $K_c$  and  $n$  are parameters depending on the geometry of the contact and on the materials. It must be pointed out that the exponent  $n$  is strictly greater than 1. It also has to be noticed that the indentation depth might include a non-elastic part. In the case considered here, this non-elastic part is included in the global non-elastic deflection  $f_{ne}$  as explained above.

It is reasonable to assume that all materials used in the device have a linear elastic behaviour before exhibiting a non-elastic one due to damage or plasticity. Thus, the suitable elastic stiffness  $K_{su}$  of the set-up can be defined:

$$P = K_{su} f_{su} \quad (4)$$

The elastic stiffness of the sample ( $K_e$ ) is defined in the same manner. Moreover, it is obvious that the non-elastic part of the total deflection measured is not recovered during the unloading. That means that the plastic part  $f_{ne}$  of the total deflection  $f$  is not involved in equation (2) during the unloading phase. This leads to the equation:

$$\left( \frac{df}{dP} \right)_{dP \leq 0} = \frac{1}{K_{su}} + \frac{1}{K_e} + \frac{1}{nK_c^{1/n}} \left( \frac{1}{P/2} \right)^{1-n} \quad (5)$$

Whatever is the contact stiffness, the third part significantly becomes smaller than the second part when the force increases. It is essential to point out that the effect of the elastic return of the contact can be neglected when the force and the contact stiffness are high enough. Moreover, the first term of the equation 5 can also be neglected for a set-up being rigid enough (i.e. very high stiffness). Hence, the elastic stiffness of the material is roughly equal to the total stiffness during the unloading phase. As a result, Young's modulus can be accurately determined from the beginning of the unloading phase as:

$$E = \left( \frac{dP}{df} \right)_{dP \leq 0} \frac{1}{8bh^3} (L-l) (2L^2 + 2Ll - l^2) \quad (6)$$

where  $(dP/df)_{dP \leq 0}$  is the slope of the curve at the beginning of the unloading.

#### 4 Application and validation of the proposed method

A program has been developed to determine the elastic modulus using the previously proposed method. The program performs two main steps: The first step detects the change of loading to find out the point

where the unloading begins ( $dP \leq 0$ ). Secondly, the slope is determined by numerical interpolation. Finally, the Young's modulus is deduced by means of equation 6. This program has been initially applied to the alumina alloy bending test. The values of modulus depending on the unloading are exhibited in the second row of the Table 2. The third row lists the values obtained by a classical linear interpolation of the monotonic curve. The usual value for this material is given in the last row. The monotonic modulus is reduced by 21 % in comparison to the usual value (70 GPa) while the modulus calculated from the unloading part tends to the usual value. The data support the assumption presented above. For the first loops crushing effect is still significant even during unloading, and the Young's modulus is underestimated as expected. From the fourth loop MOE fairly remains stable at 70 GPa in accordance with the usual value. As a result, it supports that the higher the force, the more accurate the evaluation of the modulus. Moreover, while the hysteretic behaviour of unloading-loading cycles reduces during the cycles, the

Table 2 • Young's modulus for alumina computed from four-point cyclic bending test

Unloading number	Young's modulus / GPa	Young's modulus deduced from apparent stiffness / GPa	Usual Young's modulus / GPa
1	43	55	70
2	55		
3	65		
4	68		
5	71		
6	71		
7	76		



**Table 3 • Young's modulus (in GPa) determined with unloading slope compared with ultra-sonic test of the two considered materials**

Material	SF60	HSC90
Test temperature / °C	800	800
Ultrasonic test	50	150
unloading slope	20 / 25 / 28 / 32 / 38 / 40	53 / 123 / 125 / 135 / 137 / 141

gap between successive modulus values decreases.

The method has been also applied to the two refractory materials presented in the previous section. Seven loops have been performed for both materials. The difference of the maximal force between two successive unloads is about 1 kN. SF60 has been tested at a temperature of 800 °C (Fig. 3) performing seven loops. The force reached a maximum of 10 kN. The elastic modulus has been calculated for each peak. The values are shown in Table 3. As expected, the MOE has a very low value for the first loops due to the crushing effect, but rises up to about 40 GPa. Assuming that the last value of MOE obtained with the proposed method is the more accurate value, it is reduced by 20 % in comparison to the modulus obtained with an ultra-sonic test [12] equal to 50 GPa. It is obvious that a MOE deduced from the apparent stiffness should give a larger difference with ultra-sonic modulus. Regarding the HS90, this material has been tested at a temperature of 800 °C. At this temperature and after the first unloading (i.e. as soon as the force has reached a level being high enough), when the crushing effect can be neglected, the modulus reveals a gradual increase from 120 to 140 GPa. For this last material considered here, the values determined with the presented method are in good agreement with MOE measured by means of ultrasonic test (150 GPa).

## 5 Conclusions

Although over the past years a lot of research has been devoted to experimental bending set-up and improvement of the

measurement device in order to correct the accuracy in MOR and MOE evaluation, Young's modulus determination reveals a common discrepancy of 10 to 30 % compared with the values obtained by tensile tests or ultrasonic measurements. This paper highlights the main reason of this error: The modulus usually determined by the monotonic loading test actually is an apparent modulus, because the non-elastic behaviour cannot be taken into account. As shown, cyclic test provides many more characteristics of the behaviour, but it is more difficult to process. Indeed, without an accurate analysis of the test, processing the data leads to an estimation of the modulus in a poor agreement compared with other methods. Moreover, to achieve results by applying the cyclic test needs obviously more time than executing the monotonic test. Hence, most studies devoted to the bending tests aim to mainly improve the set-up, thereby avoiding the non-linear characteristic of the force-deflection curve. On the contrary, the authors rather advocate the use of cyclic test. They propose to accept the device as such and to process data taking into account this specific behaviour.

While the deflection record during the monotonic loading test is a complex sum of many effects, the record of the elastic return during unloading enables the accurate determination of the elastic behaviour of the sample. Indeed, at the beginning of the unloading, the part of the deflection return mainly is driven by the sample stiffness. Using this consideration, the authors have developed a program which uses the beginning of the unloading to estimate the

Young's modulus. Results obtained are in good agreement with the results obtained by using other techniques. The results determined for the alumina reference material support the assumptions presented here. Tests carried out on refractory materials gave a deviation with ultrasonic measurement lower than 20 %.

## References

- [1] Blond, E., Schmitt, N., Hild, F., Poirier, J., Blumenfeld, P.: Modelling of high temperature asymmetric creep behaviour of ceramics. *J. Eur. Ceram. Soc.* 25 (2005) [11] 1819-1827
- [2] Schmitt, N., Berthaud, Y., Poirier, J.: Tensile behaviour of magnesia carbon refractories. *J. Eur. Ceram. Soc.* 20 (2000) [12] 2239-2248
- [3] Bazant, Z. P., Pijaudier-Cabot, G.: Measurement of characteristic length of non-local continuum. *J. Eng. Mech., ASCE.* 115 (1985) [4] 755-767
- [4] Mazars, J., Berthaud, Y.: Une technique expérimentale appliquée au béton et pour créer un endommagement diffus et mettre en évidence son caractère unilatéral. *Comptes Rendus Acad. Sci.* 308 (1989) [série II] 579-584 (in French)
- [5] Nazaret, F., Marzagui, H., Cutard, T.: Influence of the mechanical behaviour specificities of damaged refractory castables on the Young's modulus determination. *J. Eur. Ceram. Soc.* 26 (2006) [8] 1429-1438
- [6] Krautkramer, J., Krautkramer, H.: Ultrasonic testing of materials, 2<sup>nd</sup> ed. Springer Verlag, Berlin, Heidelberg, New York 1977
- [7] Baudson, H. et al.: Ultrasonic Measurement of Young's modulus MgO/C refractories at high temperature. *J. Eur. Ceram. Soc.* 19 (1999) [10] 1895-1901
- [8] Robert, L. et al.: Use of 3-D Digital Image Correlation to Characterize the Mechanical Behaviour of a fiber Reinforced Refractory Castable. *Exp. Mech.* 47 (2007) [6] 761-773
- [9] Advanced technical ceramic. Mechanical properties of monolithic ceramics at room temperature - Part 1: Determination of flexural strength. NF EN 843-1. Paris, Afnor 2007
- [10] Timoshenko, S.: Strength of materials. D. Van Nostrand Company, Princeton, New Jersey 1955
- [11] Advanced technical ceramic. Thermomechanical properties of monolithic ceramics - Part 5: Determination of elastic moduli at elevated temperatures. NF EN 820-5. Paris, Afnor 2009
- [12] Bahloul O.: PhD thesis. University of Limoges, France 2009
- [13] Johnson, K.L.: Contact mechanics. Cambridge University Press 1985. ISBN: 0-521-34796 3
- [14] Aublin, M.: Systèmes mécaniques, Dunod, DL, Paris 2005. ISBN: 2-10-049104-0